Numerical Comparison of Hydraulic Characteristics in KAERI 61-PIN Wire-Wrapped Fuel Assembly using STAR-CCM+ and ANSYS CFX

Gi-Uk Choi[a], Jonggan Hong[b], Yo-Han Jung[b], Jae-Ho Jeong[a*]
[a]*Gachon University, 1342, Seongnam-daero, Sujeong-gu, Seongnam-si, Gyeonggi-do*
[b]*Korea Atomic Energy Research Institute, 111 Daedeok-daero, 989 Beon-gil, Yuseong-gu, Daejeon 34057*
[*]*Corresponding author: jaeho.jeong@gachon.ac.kr*

1. Introduction

Gen-IV SFR (Sodium-cooled Fast Reactor) is a reactor that uses fast neutrons to generate fission reactions and transfers heat using sodium as a coolant. SFR has attracted a lot of attention from several countries as a solution to the problem of sustainable energy supply, because it is compact and has high power density. Recently, development of computational performance and computational analysis has made it possible to study computational fluid dynamics of SFR fuel bundles. In the field of high-fidelity CFD analysis, research institutes and universities around the world are establishing CFD-based analysis methodologies for fuel assembly. ANL(Argone National Laboratory) developed NEK5000 CFD code for nuclear fuel assembly, performed LES (Large Eddy Simulation) analysis, and RANS(Reynolds-Averaged Navier–Stokes equations) analysis using STAR-CCM+ commercial CFD code [1,2]. JAEA (Japan Atomic Energy Agency) developed SPIRAL's proprietary CFD code and performed RANS-based high-fidelity thermal fluid analysis [3].

The fuel assembly of the SFR consists of a fuel rod wrapped with wire around the fuel rod. For compact support, rods are placed in a triangular arrangement on a hexagonal duct. Wire-wrap around fuel rods create complex and periodic flow fields. Ginsberg [4], Cheng and Todreas [5], Lafay [6] et al. conducted a study to quantify the thermal-hydraulic performance under various SFR core and operating conditions. In addition, the subchannel analysis code evaluate the local thermal-hydraulic behavior of the fuel assembly. In a sub-channel analysis code, mass, momentum and energy conservation equations are modeled and solved together with initial and boundary conditions [8]. Since the wire complicates the flow distribution of axial and transverse flows, verification of the velocity distribution in the subchannel is required.

Many previous studies have been conducted in order to investigate the thermal-hydraulic behavior of nuclear fuel assemblies, using various turbulence models of computational fluid dynamic [8,9,10]. However, very few studies investigate the thermal behavior of fuel assemblies at full scale using the SST turbulence model. In the present study, the CFD was verified based on the experimental data of the 61-pin test assembly conducted by the KAERI [11]. And, the thermal hydraulic behavior of fuel assemblies was compared using the computational fluid dynamics codes STAR-CCM+ and ANSYS CFX. The RANS based CFD methodology is implemented with high resolution scheme in convection term and SST (Shear Stress Transport) turbulence model in the 61-pin wire-wrapped fuel assembly of KAERI.

2. Numerical method

2.1 Computational grid system

In order to insure a correct modeling, the meshes in the contact region between rod and wire spacer, a shape on the contact region should be sustained without displacement. However, wire-wrapped fuel assembly is the numerous contact lines and points between pins and wires that make the geometry complex to generate, and the computational mesh difficult to generate. The spiral wire spacer when creating the mesh makes it difficult to explain the point contact shape between the rod and the wire spacer.

For the high-fidelity computational fluid dynamics of complex core nuclear fuel assembly, it is necessary to implement without distortion of geometry. An innovative grid generation method using Fortran-based in-house code was applied [12]. Because the actual wire shape is simulated without distortion of the shape, the prediction of the contact area between the wire and the rod can be made more accurately. Simulation results using this methodology have been proven that it is possible to accurately predict the pressure drop and flow analysis of the nuclear fuel assembly [8].

The grid that composes around the rod and wire is called inner fluid domain. And the grid system of the region surrounding the repeated inner fluid is called outer fluid domain. In this way, the point contact between the wire and the rod was precisely simulated. Fig. 1 shows the computational grid configuration of the KAERI 61-pin fuel assembly, it is composed of 26 million hexahedron elements. The same grid system in Fig. 1 was used for STAR-CCM+ and ANSYS CFX.

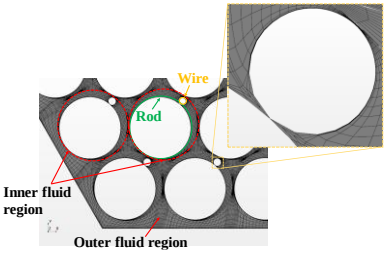

Fig. 1. Computational grid system of the KAERI 61-pin fuel assembly

2.2 Test section

KAERI has conducted a conceptual design of the PGSFR [13]. The 61-pin fuel assembly of the KAERI was designed to verify the flow characteristics of the PGSFR 217-pin fuel assembly. A downscaled experiment for the thermal-hydraulic simulation of the prototype was designed considering the geometrical similarity and the flow-dynamic similarity to preserve the hydraulic properties [14]. In order to maintain the geometrical similarity between the 61-pin test assembly and the PGSFR assembly, the configuration of the test assembly was designed to be the same as the prototype. Therefore, the parameters P/D and H/D that have the greatest influence on the flow characteristics of the subchannel is same [11]. The major design parameters are summarized in Table I.

Table I. Geometric information of fuel assembly

Geometry Parameters	Values
Number of pins	61
Pin diameter	8 mm
Wire diameter	1 mm
Wire lead pitch	238.9 mm
Pin pitch	9.12 mm
P/D	1.14
H/D	29.86
Total length	1500 mm
Working fluid	Water at 60 ºC
Density	983.2 kg/m^3
Dynamic viscosity	4.61E-4 Pa-s

2.3 Boundary condition

Table II. shows the boundary conditions for CFD analysis. The inlet is defined as a mass flow rate of various values and the outlet is defined as a constant outlet pressure of 0 Pa. The surface of the rods and wire spacers is defined with a no-slip condition with a smooth roughness. The duct wall is also applied under a no-slip condition with a smooth roughness.

Table II. Boundary condition of CFD analysis

Boundary domain	Condition	Value
Inlet	Mass flow rate	Variable [kg/s]
Outlet	Relative pressure	0 [Pa]
Rod wall	No slip	-
Wire wall	No slip	-
Duct wall	No slip Adiabatic	-

2.4 Turbulence model

Three major numerical analysis techniques can be used for turbulent flow fields: direct numerical simulation (DNS), large eddy simulation (LES), and Reynolds-averaged Navier-Stokes (RANS) simulation. RANS uses time-based, ensemble-averaged Navier-Stokes equations and models all of the effects from turbulence. Although RANS yields a lower resolution of analysis than DNS or LES, it is widely used in engineering applications due to the practical aspect of not requiring high-resolution calculation grids. The turbulence models for the RANS equations are for computing the Reynolds stresses tensor from the turbulent fluctuations in the fluid momentum. Considering computational resources, the computational cost of DNS and LES increases with the cube and square of the Reynolds number. Therefore, in the CFD analysis of this study, a RANS simulation was adopted. The turbulence models such as k-ε, k-ω, and SST have become industry standard models and are commonly used for most types of engineering problems. The SST model solves the above problems for switching to the k-ε model in the free-stream and the k-ω model in the viscous sublayer [10]. Sensitivity studies of turbulence models such as Reynolds Stress Model (RSM), k-ε, k-ω and SST were performed on a 127-pin fuel assembly. In that study, the friction factors with the SST model are 1.5–4.5% higher than that with the k-ε model. The friction factor with the SST model is 1.4–1.5% smaller than that with the k-ω model. Because the SST model switches to the k-ε model and the k-ω model, the value of the friction factor with the SST model is between that with the k-ε model and that with the k-ω model. The minimum grid scale on the fuel rod surface was 5.0×10^{-7} mm to capture the laminar to turbulent flow transition with the SST turbulence model, and the friction velocity y+ is approximately close to 2.5. In this study, the SST model of CFD was used for investigation.

2.5 Sensitivity studies of wall grid scales and turbulence model

ANSYS CFX and STAR-CCM+ have built-in various turbulence models such as k-ε, k-ω, Reynolds Stress Turbulence, and Spalart-Allmaras Turbulence. It is necessary to analyze the sensitivity of the model. The k-ε turbulence model accurately predicts turbulence behavior in the free turbulence region where the pressure gradient is small, but the boundary layer separation prediction in the viscous low layer region is inaccurate. Wilcox's k-ω turbulence model accurately predicts delamination due to reverse pressure gradients, but is sensitive to inflowing free turbulence. Therefore, Menter proposed the SST model using only the advantages of the k-ε and k-ω turbulence models. In this study, in order to understand the sensitivity of STAR-CCM+, studied the sensitivity to three turbulence models such as k-ε, k-ω, and SST.

Fig. 2 is a graph showing the result of comparing the CFD result of the fuel assembly by the turbulence model and the friction factor of the 61-pin fuel assembly of the experimental correlation equation. The experimental

correlation equations compared are Rehme correlation (1973), Upgraded Cheng and Todreas Detailed correlation (2018), and Cheng and Todreas Simpled (1986), and the equations are as follows. For all Reynolds number ranges and all turbulence models, the error between the upgraded Cheng and Todreas detailed (UCTD) occurred within 5%. In addition, the *k-ω* turbulence model and the SST turbulence model were most accurately predicted under the actual operating conditions.

Fig. 3 shows the grid sensitivity results for the axial grid spacing, and Fig. 4 shows the grid sensitivity for the y+ value. As the y+ value based on wall-normal grid spacing directly influence calculation of w specific dissipation rate value in *k-ω* turbulence model, different grids having various y+ values were compared. The stream-wise and radial grid-spacing is also compared to confirm whether different stream-wise and radial grid-spacing induce different analysis results. Coarse axial grids increase discretization errors. The pressure drop value of normalized streamwise grid scale 10 was inaccurately predicted because the coarse axial grid increases discretization error [15]. Therefore, it is necessary to dense the axial grid above a certain level.

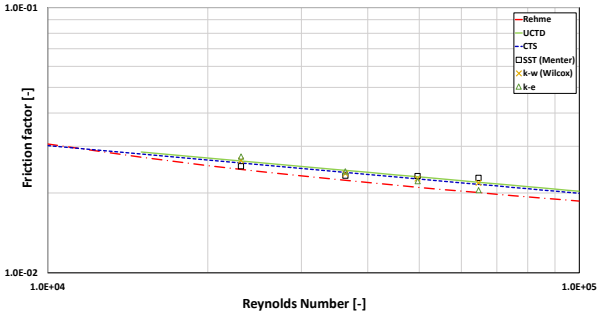

Fig. 2. Friction factors with RANS based different turbulence models

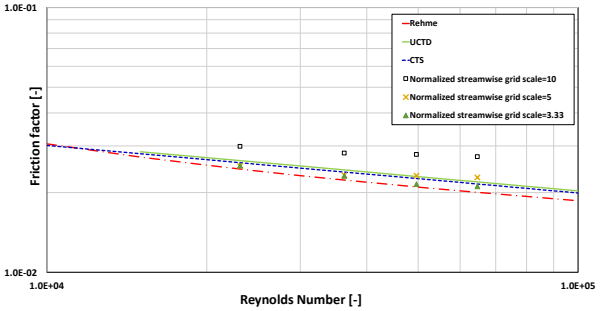

Fig. 3. Friction factors with different axial grid scales

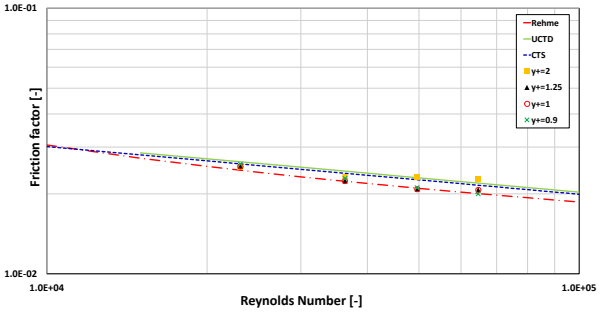

Fig. 4. Friction factors with different wall grid scales

In the present study, we conducted a steady RANS simulation with the SST turbulence model with grid which has y+ of 2, normalized streamwise grid scale of 5 to investigate the three-dimensional and vortical flow phenomena in STAR-CCM+ and ANSYS CFX. A high-resolution scheme was used for the convective term. Convergence of the simulation was judged based on the periodic pressure on the outlet domain of the 61-pin fuel assembly. In addition, the CFD analysis results closest to the experimental results were selected in order to understand the flow phenomenon.

3. Code to code comparison

To verify the analysis result with STAR-CCM+, we performed code to code comparison verification with ANSYS CFX. In previous studies, high-fidelity CFD flow analysis of fuel assembly using ANSYS CFX was conducted for 7-pin, 19-pin, 37-pin, 61-pin, 127-pin, 217-pin fuel assembly, and was verified through experimental data and experimental correlations. Therefore, the verified calculation results of ANSYS CFX were used and compared with the STAR-CCM+ results. STAR-CCM+ and ANSYS CFX performed computational fluid analysis using the same boundary conditions and grids. The automatic grid generator for each code varies greatly from code to code, depending on the type of mesh element. Therefore, the grid system described in Section 2.1 was used in the same way for accurate comparison.

3.1 Comparison of pressure drop

Many researchers have conducted experiments to derive the friction factor correlation of wire-wrapped rod bundles. The pressure drop on fully developed flow is calculated as follows:

$$f = \Delta P \frac{D_h}{L} \frac{2}{\rho V^2} \quad (1)$$

Rehme[16], Engel[17], Cheng, and Todreas[18,19] have compared the correlations of the friction factor of fuel assembly in various Reynolds number ranges in detail and evaluated the applicable ranges. Eqs. (2)-(5)

show the relational expressions. It is important to determine the appropriate correlation equation to use for the SFR fuel rods and applicable ranges. The validity range of the friction factor correlation are summarized in Table III [20].

Table III. Application range and database for friction factor correlations

Model	N_r	P/D	H/D	Re	Uncertainty
Rehme	7-217	1.1-1.42	8.0-50.0	1000-3×10^5	±8%
Engel	19-61	1.067-1.082	7.7-8.3	All regimes (50-10^6)	±15%
CTS	19-217	1.025-1.420	8.0-50.0	All regimes (50-10^6)	Not evaluated
UCTD	7-271	1.000-1.420	8.5-52.0	All regimes (50-10^6)	Not evaluated

The Rehme(1973) correlation

$$f = \left(\left(\frac{64}{Re}\right)F^{0.5} + \left(\frac{0.0816}{Re^{0.133}}\right)F^{0.9335}\right)(Nr)\pi(D + D_w)/St \quad (2)$$

Where:

$$F = (P/D)^{0.5} + (7.6(P/D)^2\ (D + D_w)/H)^{2.16}$$

The Engel(1979) correlation

$$Laminar\ flow: f = \frac{110}{Re}\ for\ Re \le 400 \quad (3).1$$

$$Turbulent\ flow: f = \frac{0.55}{Re^{0.25}}\ for\ Re \ge 5000 \quad (3).2$$

The Simplified Cheng and Todreas(1986) correlation

$$Laminar\ flow: f = \frac{C_{fL}}{Re}\ for\ Re \le Re_L \quad (4).1$$

$$Turbulent\ flow: f = \frac{C_{fT}}{Re^{0.18}}\ for\ Re_T \le Re \quad (4).2$$

Where:

$$Re_L = 300(10^{1.7(P/D-1.0)})$$

$$Re_T = 10{,}000(10^{0.7(P/D-1.0)})$$

$$C_{fL} = (-974.6 + 1612.0(P/D) - 598.5(P/D)^2)(H/D)^{0.06-0.085(P/D)}$$

$$C_{fT} = \left(0.8063 - 0.9022(log\ H/D)\right) + 0.3526(log(H/D)^2) * (P/D)^{9.7}\ (H/D)^{1.78-2.0(P/D)}$$

The Detailed Upgraded Cheng and Todreas(2018) correlation

$$Laminar\ flow: f = \frac{C_{fL}}{Re}\ for\ Re \le Re_L \quad (5).1$$

$$Turbulent\ flow: f = \frac{C_{fT}}{Re^{0.18}}\ for\ Re_T \le Re \quad (5).2$$

Where:

$$C_{fL} = De_b\left(\sum_{i=1}^{3}\left(\frac{N_i A_i}{A_b}\right)\left(\frac{De_i}{De_b}\right)\left(\frac{De_i}{C_{fiL}}\right)\right)^{-1}$$

$$C_{fT} = De_b\left(\sum_{i=1}^{3}\left(\frac{N_i A_i}{A_b}\right)\left(\frac{De_i}{De_b}\right)^{0.0989}\left(\frac{De_i}{C_{fiT}}\right)^{0.54945}\right)^{-1.82}$$

Where i = b, 1, 2 or 3 for bundle average, interior, edge and corner subchannel.

Fig. 5 shows a comparison of the 61-pin fuel assembly CFD analysis results with the friction factor correlations. The CFD result was the best fit with the UCTD relational expression. It has been reported that the UCTD relation is the most desirable for the best accuracy of the pressure drop analysis of wire-wrapped fuel rod bundles. In nominal operating flow (Re ≈ 65,000), ANSYS CFX and STAR-CCM+ overestimated the UCTD correlation by about 4%. STAR-CCM+ and ANSYS CFX had a large difference from the experience correlation under low flow rate conditions. There are sections where transitions occur under low flow conditions, and it is difficult to predict accurate pressure drop with existing turbulence models. In the experimental results under the same flow rate conditions, a pressure drop of 0.488 MPa occurred [21], and in the CFD result, a pressure drop of 0.500 MPa occurred, showing an error of 2.4%.

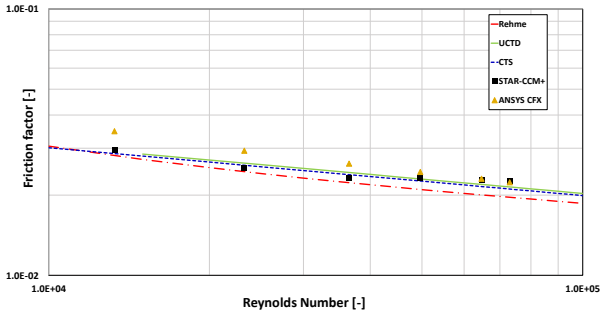

Fig. 5. Friction factors with different CFD code

3.2 Comparison of flow phenomenon

Complicated and vortical flow phenomena in the wire-wrapped fuel bundles have been elucidated by a CFD analysis with a high resolution scheme and a shear stress transport (SST) turbulence model, and by a vortex structure identification technique based on the critical point theory [22].

As shown in Fig. 6, the relative position of the vortex in each sub-channel is closely related to the vortex structure behavior and the three-dimensional flow phenomenon. The edge, corner, and interior vortex structures are periodically changed according to the relative positions of the wire spacer and the duct. The edge vortex structure has a larger axial velocity than other vortexes structure, and the edge vortex structure is a type of longitudinal vortex and has a larger scale than other sub-channels. The strong longitudinal vortex structure in the edge sub-channel can achieve better heat transfer characteristic than in the corner and interior sub-

channels. The vortex structure affects the heat transfer characteristics. STAR-CCM+ and ANSYS CFX predict these vortex structure and flow phenomenon well.

Fig. 7 shows a visualization of the vortex structure in interior subchannel of the intermediate section. As mentioned above, the vortex structure changes periodically according to the relative positions of the wire spacer and the duct wall. Normalized helicity is defined by (6).

$$H_n = \frac{\vec{\zeta} \cdot \vec{\omega}}{|\zeta| \cdot |\omega|} \quad (6)$$

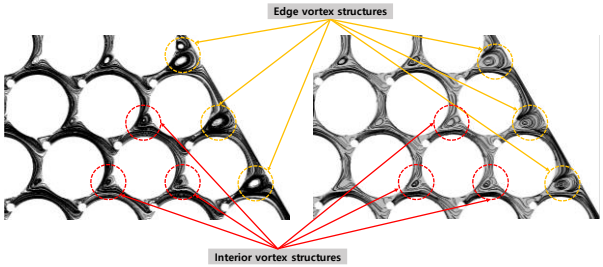

(a) STAR-CCM+ (b) CFX

Fig. 6. Vorticity of each CFD code in intermediate section

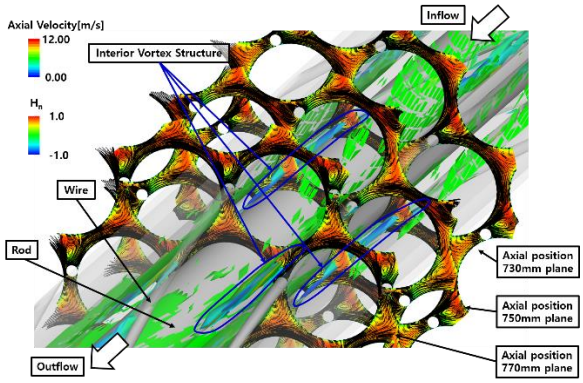

Fig. 7. Vortex core distribution and vorticity

As shown in Fig. 8, the velocity component and the turbulent kinetic energy were compared at the interior Sc2 of STAR-CCM+ and ANSYS CFX. The subchannel numbers are shown in Fig. 9. In the case of axial velocity, it is observed almost the same, it can be seen that the low speed region due to the wake of the wire appears periodically at the peak point. However, there was a slight difference between the velocity u and the velocity v. It is because the turbulence kinetic energy in STAR-CCM+ is calculated to be larger. In addition, the variability of turbulent kinetic energy is even greater.

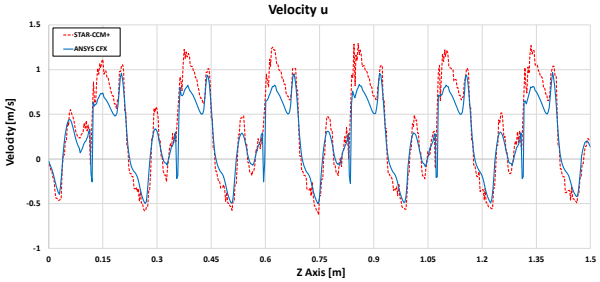

(a) Velocity u of each CFD code at point

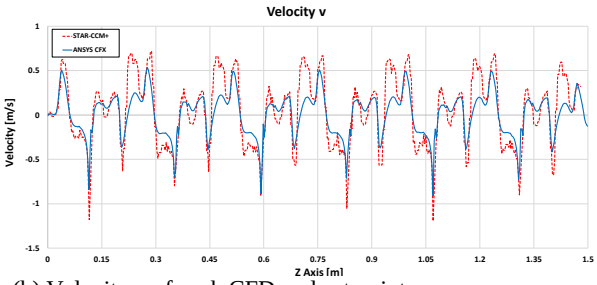

(b) Velocity v of each CFD code at point

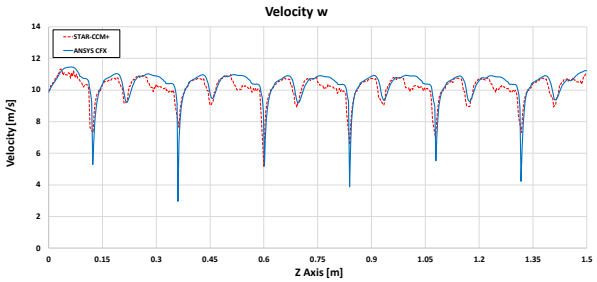

(c) Velocity w of each CFD code at point

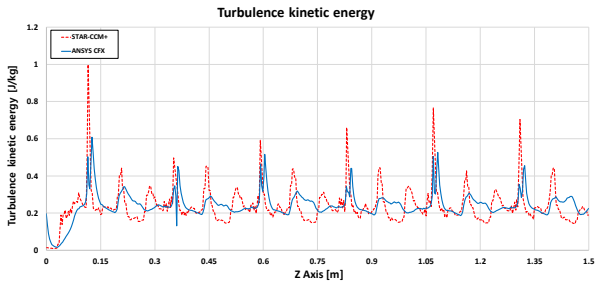

(d) Turbulence kinetic energy of each CFD code at point

Fig. 8. Comparison of velocity components and turbulence kinetic energy

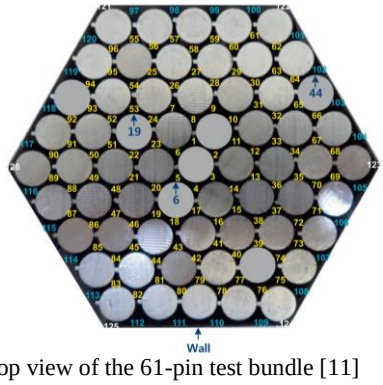

Fig. 9. Top view of the 61-pin test bundle [11]

4. Conclusion

The hydraulic phenomena in a 61-pin a wire-wrapped fuel assembly of KAERI 61-pin test assembly with the nominal operating flow value was elucidated with CFD simulation using STAR-CCM+ and ANSYS CFX. This study was conducted to evaluate the suitability and performance of the CFD codes for simulating wire-wrapped fuel assembly. According to the results of the CFD investigation, the conclusions are as follows:

1. Sensitivity analysis was performed according to the flow rate, and the results are as follows:
- Turbulence model sensitivity analysis of *k-ε, k-ω*, and SST was performed, and the SST model matched the UCTD correlation best.
- Grid sensitivity analysis was performed for the axial grid and the wall grid.
2. The pressure drop values of STAR-CCM+ and ANSYS CFX were compared under various flow rates, and they agreed with the UCTD correlation, and a difference of 2.4% between the two codes occurred at the normal operating flow rate.
3. Three-dimensional flow distributions were analyzed in the same plane and position and showed the same vortex structure. Also, the vortex structure in interior subchannel was visualized using the vortex visualization technique.
4. Based on the STAR-CCM+ methodology developed in this study, plan to perform thermal-hydraulic data validation on the PNC 37-pin fuel assembly [23,24]. In addition, CFD benchmark study in the transition region with relatively high uncertainty will be performed.

ACKNOWLEDGMENTS

This work was supported by Korea Institute of Energy Technology Evaluation and Planning(KETEP) grant funded by the Korea government(MOTIE) (No. 20214000000780, Methodology Development of High-fidelity Computational Fluid Dynamics for next generation nuclear power) and This work was supported by the National Research Foundation of Korea(NRF) grant funded by the Korea government(MSIT) (No. 2021M2E2A2081062)

REFERENCES

[1] E. Merzari, P. Fischer, M. Min, S. Kerkemeier, A. Obabko, D. Shaver, H. Yuan, Y. Yu, J. Martinez, L. Brockmeyer, L. Fick, G. Busco, A. Yildiz, Y. Hassan, "Toward exascale: overview of large eddy simulations and direct numerical simulations of nuclear reactor flows with the spectral element method in Nek5000", Nuclear Engineering and Technology, pp.1-17, 2020
[2] Merzari, E., Pointer, W.D., Smith, J., G, Tentner A, Fischer P, "Numerical simulation of the flow in wire-wrapped pin bundles: effect of pin-wire contact modeling". Nuclear Engineering and Design, vol.253, pp. 374–386, 2020
[3] R. Yoshikawa, Y. Imai, N. Kikuchi, M. Tanaka, A. Gerschenfeld, "Validation study of finite element thermal-hydraulics analysis code SPIRAL to a large-scale wire-wrapped fuel assembly at low flow rate condition", Proceedings of Joint International Conference on Supercomputing in Nuclear Applications + Monte Carlo, 2020
[4] Ginsberg, T., "Forced-flow interchannel mixing model for fuel rod assemblies utilizing a helical wire-wrap spacer system", Nuclear Engineering and Design, vol.22 (1), pp. 43-50, 1972
[5] Cheng, S.-K., Todreas, N.E., "Hydrodynamic models and correlations for bare and wire-wrapped hexagonal rod bundles — bundle friction factors, subchannel friction factors and mixing parameters" Nuclear Engineering and Design, vol.92 (2), pp. 227-251, 1986
[6] Lafay, J., Menant, B., Barroil, J., "Local Pressure Measurements and Peripheral Flow Visualization in a Water 19-Rod Bundle Compared with FLICA II B Calculations: Influence of Helical Wire-Wrap Spacer System". CEA-CONF, 1975
[7] Steward, C.W., Wheeler, C.L., Cena, R.J., "COBRA-IV: the model and the method. In: Battelle Pacific Northwest Laboratories Richland", Washington, USA, 1977
[8] Jae-Ho Jeong, Min-Seop Song, Kwi-Lim Lee, "RANS based CFD methodology for a real scale 217-pin wire-wrapped fuel assembly of KAERI PGSFR", Nuclear Engineering and Design, vol. 313, pp,.470-485, 2017
[9] Gajapathy, R., Velusamy, K., Selvaraj, P., et al. "CFD investigation of effect of helical wire-wrap parameters on the thermal hydraulic performance of 217 fuel pin bundle", Annals of Nuclear Energy, vol. 77, pp. 498–513, 2015
[10] Pointer, W.D., Thomas, J., Fanning, T., Fischer, P., Siegel, A., Smith, J., Tokuhiro, A. "RANS-based CFD Simulation of Sodium Fast Reactor Wire-wrapped Pin Bundles.", M&C, Saratoga Springs, USA, 2009
[11] Seok-Kyu Chang, Dong-Jin Euh, Seok Kim, Hae Seob Choi, Hyungmo Kim, Yung Joo Ko, Sun Rock Choi, Hyeong-Yeon Lee, "Experimental study of the flow characteristics in an SFR type 61-pin rod bundle using iso-kinetic sampling method", Annals of Nuclear Energy, 106, pp. 160-169, 2017
[12] Yamamoto, K., "An Elliptic-hyperbolic Grid Generation Method and Application to Compressor Flows.", Special Publication of National Aerospace laboratory, SP 19, pp. 193-198, 1992
[13] Yoo Jaewoon et al, "Overall system description and safety characteristics of Prototype Gen IV Sodium Cooled Fast Reactor in Korea" Nuclear Engineering and Technology, vol.48, pp. 1059-1070, 2016
[14] Euh, D.J. et al., "A flow and pressure distribution of APR+ reactor under the 4- pump running conditions with a balanced flow rate", Nuclear Engineering and Technology, vol.44, 735–744, 2012
[15] Botros N Hanna et al, "Coarse-Grid Computational Fluid Dynamic (CG-CFD) Error Prediction using Machine Learning", Journal of Fluids Engineering, 2017
[16] K. Rehme, "Pressure Drop Correlations for Fuel Element Spacers", Nuclear Technology, vol. 17, pp. 15-23, 1973
[17] F. Engel, R. Markley and A. Bishop, "Laminar, Transition, and Turbulent Parallel Flow Pressure Drop Across Wire-Wrap-Spaced Rod Bundles", Nuclear Science and Engineering, vol. 69 (2), pp. 290-296, 1979
[18] Cheng, S.K., Todreas, N.E., "Hydrodynamic models and correlations for bare and wire-wrapped hexagonal rod bundles – bundle friction factors, sub-channel friction factors and mixing parameters." Nuclear Engineering and Design, vol. 92, pp. 227-251, 1986
[19] S.K. Chena, Y.M. Chena, N.E. Todreas, "The upgraded Cheng and Todreas correlation for pressure drop in hexagonal wire-wrapped rod bundles", Nuclear Engineering and Design, vol. 335, pp. 356-373, 2018
[20] Su-Jong Yoon, Florent Heidet, "Evaluation of pressure drop correlations for the wire-wrapped rod bundles", Transactions of the American Nuclear Society, vol. 122, pp.803-806, 2020
[21] Sun Rock Choi et al., "Assessment of subchannel flow mixing coefficients for wire-wrapped hexagonal fuel rod bundles", Annals of Nuclear Energy, vol.166, 2022

[22] Jae-Ho Jeong, Min-Seop Song, Kwi-Lim Lee, "CFD investigation of three-dimensional flow phenomena in a JAEA 127-pin wire-wrapped fuel assembly", Nuclear Engineering and Design, vol. 323, pp.166-184, 2017
[23] Muhammad Enamul Kabir, Hiroki Hayafune, "Study of thermohydraulic behavior within the fuel bundle under a loss of flow condition", POWER REACTOR AND NUCLEAR FUEL DEVELOPEMENT CORPORATION, PNC TN9410 92-018, 1992
[24] Masahiko OTAKA, Hiroyuki OHSHIMA, Hisashi NINOKATA, Hitoshi NARITA, "Validation of Single-Phase Subchannel Analysis Code ASFRE-III", POWER REACTOR AND NUCLEAR FUEL DEVELOPMENT CORPORATION, PNC TN9410 96-212, 1996